THE EFFECTS OF PHYSICAL AGING ON ENTHALPY RELAXATION IN POLYMERS.

A PHENOMENOLOGICAL APPROACH

Ian M. Hodge
BFGoodrich R&D Center
Brecksville, Ohio 44141

Abstract

Experimental and computer simulation enthalpy relaxation studies of physical aging in glassy polymers are described. The effects on aging of different thermal and nonthermal histories of the glass, such as cooling rate, hydrostatic pressure, vapor absorption and desorption, and tensile stress, are discussed. The effects of the same nonthermal perturbations applied during aging, and of aging time and temperature, are also presented. Information on aging is obtained from the amount of enthalpy lost during aging and how that enthalpy is recovered during heating to above the glass transition region. The rate of aging is increased by histories which raise the excess enthalpy of the glass, reflecting the nonlinearity of the aging kinetics. Hydrostatic pressure, absorbed vapor, and mechanical stress applied during aging slow down the rate of enthalpy loss. Depending on the chemical nature and history of the glass and the aging conditions, enthalpy recovery during heating occurs in temperature ranges centered from well below to just above the glass transition range. Recovery below Tg is shown to be a manifestation of the memory effects associated with nonexponential decay functions.

Contents

1. Physical Aging

Glasses usually exist in a non-equilibrium state and relaxation towards equilibrium is commonly referred to as physical aging. Aging affects a large number of properties including but not restricted to density, enthalpy and entropy, creep compliance and modulus, dielectric permittivity and electrical conductivity. The term "physical" aging intimates that the changes in these and other properties occur in the absence of phase changes (e.g. crystallization) or chemical reactions (e.g. photochemical degradation).

Enthalpy is a convenient property to monitor physical aging with because of the availability of accurate and sensitive Differential Scanning Calorimetry (DSC) instruments. Enthalpy lost during aging is recovered during reheating to above Tg, and this recovery is usually manifested as a maximum in the heat capacity which occurs at temperatures ranging from well below to the upper edge of the glass transition region. An example of enthalpy recovery well below Tg is found in the pioneering study of PVC by Illers (1), and recovery near Tg is exemplified by the early study of PS by Volkenstein and Sharonov (2). A large body of experimental data on the effects of physical aging on enthalpy relaxation in polymers has been published (1-23) and some generalizations can be made:

(1) The effects of aging are removed on heating the glass above Tg.

(2) The temperatures (T_{max}) at which the heat capacity maxima (Cp_{max}) appear increase approximately linearly with both annealing temperature (T_e) and log(annealing time, t_e), when the aged glass is not too close to equilibrium. There are indications that T_{max} increases approximately with log(heating rate, QH) (9), although this is not well established.

(3) The magnitude of Cp_{max} increases approximately linearly with T_e and log t_e, as does the enthalpy lost during aging, ΔH_e, of which Cp_{max} is a crude measure.

(4) As the aged glass approaches equilibrium deviations from these linear relations are observed until at equilibrium no changes with aging occur. At fixed t_e, ΔH_e and Cp_{max} pass through a maximum as a function of T_e, often when T_e is about 20K below Tg, and decrease to zero when $T_e >> Tg$. At fixed T_e, ΔH_e and Cp_{max} become constant at long t_e as the aged glass approaches equilibrium.

For PVC, additional general features are found:

(5) T_{max} is insensitive to the history of the glass before aging, such as cooling rate (20), vapor induced swelling (20), hydrostatic pressure during cooling (4,16), and mechanical strain (16,20).

(6) Cp_{max} and ΔH_e are strong functions of history before aging. Histories which elevate the excess enthalpy before aging increase ΔH_e and Cp_{max}.

The reproduction of these trends is an essential test of computer simulations of physical aging.

2. Phenomenology

The increased rate of aging as temperature approaches Tg, and the elimination of aging effects after heating to above Tg, suggest a close connection between aging and the glass transition phenomenon. This is confirmed by the successful application of glass transition phenomenology to physical aging by Kovacs and coworkers (24) and Hodge and Berens (25). In anticipation of this connection, we describe in this section the phenomenology of nonexponential, nonlinear relaxations in the glass transition region.

Glass transition kinetics are nonexponential in the sense that relaxation towards equilibrium is described by a nonexponential decay function $\phi(t)$. This is formally equivalent to a distribution of relaxation times $g(\tau)$, related to $\phi(t)$ by

$$\phi(t) = \int_0^\infty g(\tau) e^{-t/\tau} \, d\tau \qquad (1)$$

and normalized such that

$$\int_0^\infty g(\tau) d\tau = 1 \qquad (2)$$

The moments of the distribution, $\langle \tau^n \rangle$, are given by

$$\langle \tau^n \rangle = \int_0^\infty \tau^n g(\tau) d\tau \qquad \text{(for all n)} \qquad (3a)$$

$$= \int_0^\infty t^{n-1} \phi(t) dt \qquad n \geq 1 \qquad (3b)$$

$$= (-1)^{|n|} \left. \frac{d^{|n|} \phi(t)}{dt^{|n|}} \right|_{t=0} \qquad n \leq -1 \text{ (integer)} \qquad (3c)$$

There is abundant experimental evidence for nonexponential relaxation in amorphous media. One consequence of nonexponentiality which has important consequences for physical aging is the memory effect. In essence, this effect describes the observation that relaxation from a particular state depends not only on what the state is, but also on how that state was reached. A classic example of this

in polymer glasses is the volume maximum with respect to time following two temperature steps of opposite sign observed by Kovacs (26). This effect is illustrated in Fig. 1, and it is instructive to analyze it. The thermal history consists of a downward temperature step of ΔT_1 to temperature T_1 at time t_1 from a starting temperature T_o at equilibrium, and an upward step of ΔT_2 to temperature T_2 at time t_2.

The time dependence of volume for $t>t_2$ is

$$V(t) = \Delta V_1 \phi(t-t_1) + \Delta V_2[1 - \phi(t-t_2)] \qquad (4a)$$

$$= \Delta V_1 \phi[(t_2-t_1) + (t-t_2)] + \Delta V_2[1 - \phi(t-t_2)] \qquad (4b)$$

where ΔV_1 and ΔV_2 are the changes in equilibrium volume corresponding to the temperature steps ΔT_1 and ΔT_2. If $\phi(t)$ is exponential and the relaxation times at T_1 and T_2 are τ_1 and τ_2, then

$$V(t) = \Delta V_1 \exp[-\frac{(t_2-t_1)}{\tau_1} - \frac{(t-t_2)}{\tau_2}] + \Delta V_2 \{1 - \exp[\frac{-(t-t_2)}{\tau_2}]\} \qquad (5a)$$

$$= \Delta V_2 + \exp[\frac{-(t-t_2)}{\tau_2}] \{\Delta V_1 \exp[\frac{-(t_2-t_1)}{\tau_1}] - \Delta V_2\} \qquad (5b)$$

The expression in curly brackets in Eq. (5b) is independent of time so that V(t) decays exponentially and no maximum in V is observed. This is not necessarily the case if $\phi(t)$ is nonexponential. To illustrate this we use a functional form for $\phi(t)$ which has been found empirically to describe a large number of relaxation phenomena in a wide variety of amorphous material: the fractional exponential or Williams-Watts function (27)

$$\phi(t) = \exp[-(t/\tau_o)^\beta] \qquad 1 \geq \beta > 0 \qquad (6)$$

For this function the transformation from Eq. 5a to Eq. 5b cannot be made because

$$[\frac{t_2-t_1}{\tau_1} + \frac{t-t_2}{\tau_2}]^\beta \neq (\frac{t_2-t_1}{\tau_1})^\beta + (\frac{t-t_2}{\tau_2})^\beta \qquad \beta \neq 1 \qquad (7)$$

In these cases V(t) may pass through a maximum for $t>t_2$. This is illustrated in Fig. 1 where V(t) from Eqs. 4 and 6 is plotted for three values of β. The long time tails for smaller values of β seen in Fig. 1 result from longer average relaxation times: Eq. 3b gives for the first moment of the William-Watts function

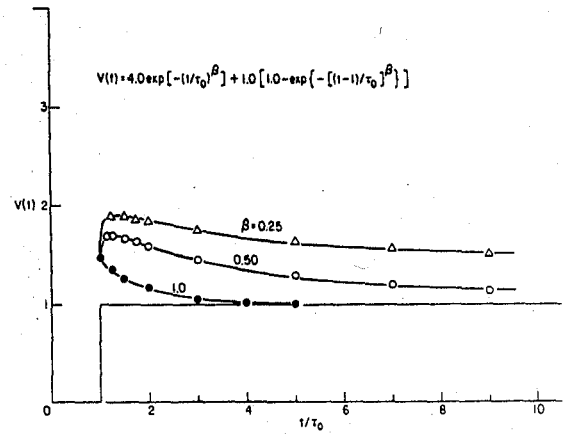

Figure One Calculated time dependences of volume following two temperature steps, for the indicated values of β (Eqs. 4,6).

$$\langle\tau\rangle = \frac{\tau_o}{\beta}\Gamma(\frac{1}{\beta}) = \tau_o\Gamma(1+1|\beta) \qquad (8)$$

where Γ is the gamma function. Thus $\langle\tau\rangle/\tau_o = 1, 2, 6$ for $\beta = 1, 0.5, 0.25$ respectively.

In addition to being nonexponential the glass transition phenomenon is also nonlinear, in the sense that the functional form of $\phi(t)$ changes with the degree of departure from equilibrium. Non-linearity can be conveniently treated by making the average relaxation time a function of "structure" as well as temperature. It is an additional convenience to treat the "structural state" of a system, as measured by a macroscopic property such as enthalpy, in terms of the fictive temperature, T_f, introduced by Toole (28). The fictive temperature of a system is the temperature at which the observed property would be the equilibrium value (usually obtained by extrapolation). Isothermal relaxation from a non-equilibrium state is then described by the decay of T_f toward T. It is worth noting that T_f measures only the relaxation component of a macroscopic property and that the fictive temperatures assessed from different properties of the same glass may differ. This is illustrated in Fig. 2 where two arbitrary properties are plotted schematically as a function of temperature. The fictive temperature of the glass immediately after cooling, T_f', is the same for each property, but because of different relaxation behavior in the transition range T_f is different for each property at the same temperature within the range. Thus glasses with the same fictive temperature arrived at by different paths may not have the same molecular configuration. The fictive temperature is a phenomenological convenience and is not an accurate measure of molecular structure.

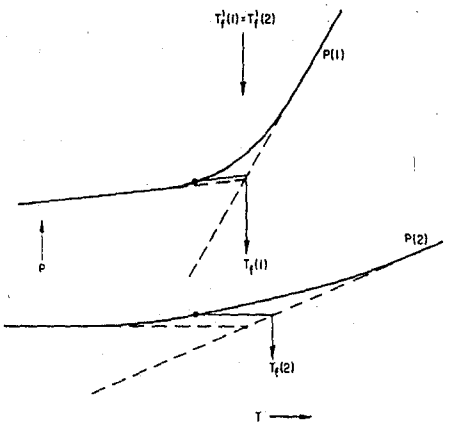

Figure Two Fictive temperature behavior for two arbitrary properties of the same material with the same thermal history.

A commonly used method for handling nonlinearity is that of Narayanaswamy and Gardon (29,30). The relaxation time (e.g. τ_o in Eq. 6) is expressed as

$$\tau_o = A \exp[\frac{x\Delta h^*}{RT} + \frac{(1-x)\Delta h^*}{RT_f}] \qquad (9)$$

where A, x, and Δh^* are constants and R is the ideal gas constant. Note that for small departures from equilibrium, $T_f \sim T$ and linear kinetics are recovered. The parameter x is a numerical measure of nonlinearity ($1 \geq x > 0$; x=1 for a linear relaxation). The parameter Δh^* determines the rate at which the frozen in fictive temperature, T_f', changes with cooling rate QC (31-33):

$$\Delta h^*/R = -\partial \ln(QC)/\partial(1/T_f')_p \qquad (10)$$

and is easily obtained from cooling rate data (see below). The preexponential parameter A is determined by Tg and Δh^*:

$$\ln A \sim -\Delta h^*/RTg + \ln \tau_o|_{Tg} \qquad (11)$$

The most important effect of nonlinearity on aging is that τ_o in non-equilibrium glasses is shortened relative to that in the equilibrium state at the same temperature, because $T_f' > T$. Thus significant decreases in T_f can occur over reasonably short times, i.e. physical aging occurs. Nonlinearity also results in self-retarding relaxation during cooling and isothermal aging, and a self-accelerating return to equilibrium during heating which may increase the heat capacity overshoot above Tg. Self retardation during aging has been shown by Struik (34) to give an approximately linear relation between log τ_o and log t_e, for an exponential relaxation.

3. Mathematical Modeling

Two basic approaches to modeling non-exponential and non-linear relaxation phenomena near and below the glass transition have been used, both of which rest on earlier work by Toole (28) and Narayanaswamy (29,30). The approach of Kovacs, Aklonis, Hutchinson, and Ramos (24) treats the non-exponential decay function as a sum of exponentials, with relaxation times and weighting factors given by summation versions of Eqs. (1) and (2). The departure from equilibrium is described by differential equations, one for each relaxation time. The resulting coupled, non-linear differential equations are solved for different thermal histories.

Another approach is due to Moynihan and coworkers (35,36). An extension of this approach to thermal histories which include aging has been described by Hodge and Berens (25), and is used here. The method treats cooling and heating as a series of temperature steps and isothermal hold times, and the response of T_f to each step is described by a decay function $\phi(t)$. As a matter of convenience and good accuracy, $\phi(t)$ is assumed to be of the Williams-Watts form although any other functional form (including a sum of exponentials) could also be used. The Narayanaswamy expression for τ_o in terms of T and T_f (Eq. 9) is used to define a reduced time t_r which is inserted into the argument of the decay function

$$t_r = \Sigma \Delta t_i/\tau_{o,i} \qquad (12)$$

where i indexes the time intervals. For cooling and heating the time intervals are the isothermal hold times between temperature steps

$$\Delta t_i = \Delta T_i/Q_i \qquad (13)$$

where ΔT_i is the temperature step and Q_i is the cooling or heating rate. The total response to cooling and heating is obtained by Boltzman superposition of responses to each temperature step. This is valid when the reduced time is used and the nonlinearity is removed by continual updating of $\tau_{o,i}$. The expression for T_f is

$$T_{f,n} = T_o + \sum_{j=1}^{n} \Delta T_j \{1 - \exp[-(\sum_{k=j}^{n} \Delta T_k/Q_k\tau_{o,k})^\beta]\} \qquad (14)$$

$$\tau_{o,k} = A \exp[\frac{x\Delta h^*}{RT_k} + \frac{(1-x)\Delta h^*}{RT_{f,k-1}}] \qquad (15)$$

where $T_{f,n}$ is the fictive temperature after n temperature steps and T_o is a starting temperature well above Tg at which equilibrium exists. For almost all of the calculations reported here constant temperature steps of 1K were used. The conditions under which this is inadequate are discussed later.

The normalized heat capacity $C_p^N(T)$ is given by dT_f/dT and is calculated from the expression

$$C_p^N(T) = \frac{T_{f,i} - T_{f,i-1}}{T_i - T_{i-1}} \qquad (16)$$

This is zero in the glassy state and unity in the rubber or liquid state.

Aging is inserted into the cooling cycle and the aging time t_e is divided into subintervals to allow for changes in T_f and τ_o (25). For most of the calculations 5 logarithmically even spaced subintervals per decade of aging time were used. During aging, Eq. (14) is modified by summing only the reduced time and truncating the Boltzman summation since no temperature steps occur during aging. The total thermal history consists of cooling at a constant rate from T_o to the aging temperature T_e, staying there for the aging time t_e, cooling again at the same rate to the minimum temperature (usually 300K) and heating at constant heating rate to well above Tg. This deviates somewhat from many experiments in which the sample is cooled to room temperature, placed in an annealing oven, cooled to room temperature again, transferred to a DSC instrument and heated. The differences appear to be negligible in most cases, however, since relaxation which occurs during transfer to and from the oven is generally small compared with that which occurs during aging. In any case for quantitative tests of the calculation procedure aging is performed in the DSC instrument, and the experimental thermal history exactly matches the history used in the calculations. The experimental variables which must be known are the cooling and heating rates and the aging time and temperature.

The use of 1K temperature steps for Boltzman integration is adequate when C_p^N does not exceed ca 2.0. For larger values of C_p^N, smaller temperature steps are required. In these cases the temperature step is varied according to C_p^N calculated for the previous step:

$$\Delta T_i = \frac{1}{C_{p,i-1}^N} \qquad C_{p,i-1}^N > 1$$

$$= 1 \qquad C_{p,i-1}^N \leq 1 \qquad (17)$$

For very large values of C_p^N this procedure may also be inadequate. However, thermal lag effects in DSC instruments would also affect these large heat capacities and quantitative comparison with experiment would therefore be difficult in any case.

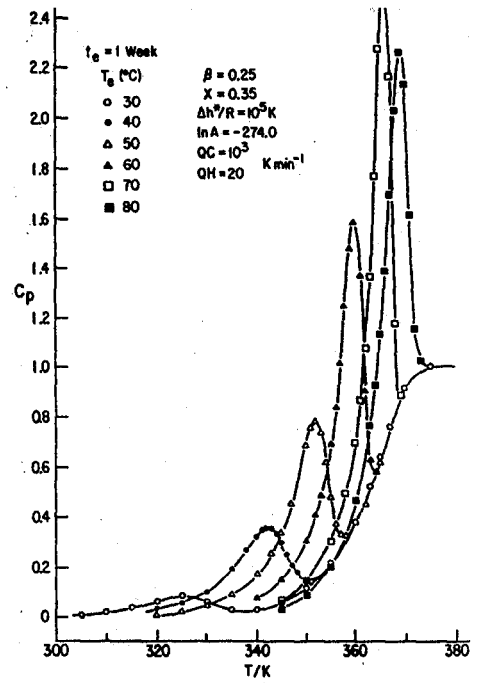

Figure Three Calculated temperature dependences of C_p^N as a function of aging temperature.

It has been shown by Hodge and Berens (25) that the calculation procedure described above reproduces all of the experimental trends listed in Section 1. As an example, we show in Fig. 3 calculated curves of C_p^N for different values of T_e at constant t_e. The experimentally observed increase in peak height ($C_{p\,max}^N$) and shift to higher peak temperatures (T_{max}) with T_e are reproduced. The peak height is calculated to pass through a maximum when $T_e \sim Tg-20$ and then decrease with T_e (observed experimentally). This maximum occurs because at low T_e the loss of enthalpy is restricted by long relaxation times, whereas at high T_e the relaxation time is sufficiently short that equilibrium can be reached ($T_f = T$) and the loss of enthalpy is determined by how much T_f' exceeds T_e at the start of aging. This excess decreases as T_e increases and eventually disappears when T_e is above Tg.

One of the more interesting effects of physical aging on enthalpy relaxation is the development of heat capacity peaks well below Tg, corresponding to enthalpy recovery in the glassy state. The earliest experimental observation of this phenomenon appears to be that of Illers (1) for PVC, and it has since

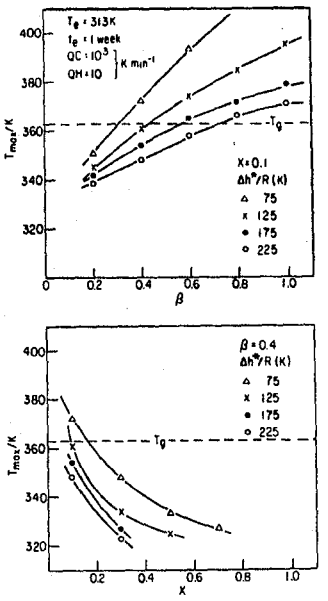

Figure Four Dependences of T_{max} on β and x for the indicated values of Δh^*. Parameter A varied with Δh^* to keep Tg fixed at 363K.

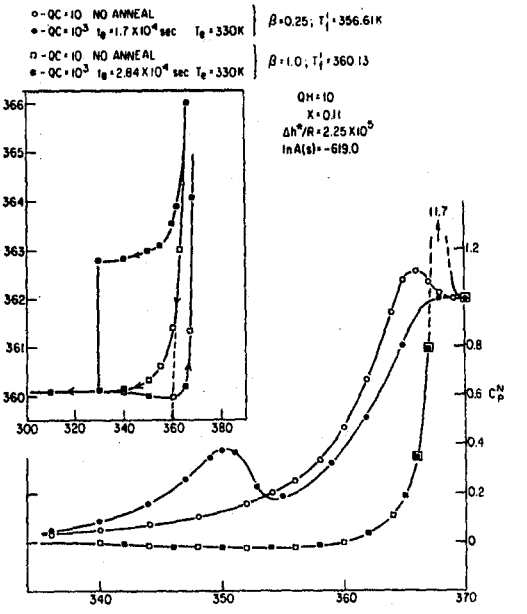

Figure Five Calculated temperature dependencies of C_p^N for a slow cooled and fast quenched plus aged glass for β = 0.25 and 1.0. Inset: Thermal histories expressed as T_f vs T.

been observed by others for PVC (3,5,15,20,37,39,41), PS (4,9,13,17,38,60,43,-44), and PMMA (22,41,42). The first theoretical explanation in terms of the glass transition kinetics was given by Kovacs et al. (24). Here we discuss the phenomenon in terms of the calculation procedure described above. First we establish the combinations of material parameters which produce sub-Tg peaks by calculating the effects of the parameters x and β for different values of Δh^*. The pre-exponential factor A is varied with Δh^* to keep Tg constant. The results are shown in Fig. 4. Low values of β and high values of Δh^* and x favor peaks below Tg. For β=1 no combination of parameters or thermal histories could be found which produced a sub-Tg peak, suggesting that the memory effect associated with non-exponential decay functions is essential for sub-Tg peak development. This is confirmed by calculated heat capacity scans of two glasses with the same T_f' arrived at by different paths: a slow cool, and a rapid quench followed by aging. These histories are displayed in Fig. 5 inset in the form of T_f vs. T plots. The corresponding heat capacity curves are shown in Fig. 5 for β = 0.25 and 1.0. For β=1 the two histories produce identical curves, corresponding to the absence of any memory effect for an exponential decay function. For β=0.25 the slowly cooled glass exhibits an overshoot above Tg and the aged glass a sub-Tg peak. The sub-Tg peak is analogous to the volume maximum following two temperature steps, observed by Kovacs (51) and discussed above, because cooling, aging, and heating are qualitatively similar to two temperature steps separated by a waiting time (the times for cooling and heating are short compared with the aging time). In both cases the glass "remembers" the aging time or time between temperature steps when β≠1.

The lowering of T_{max} with increasing Δh^* and x also occurs for shorter aging times and lower aging temperatures. These variations in parameters and aging conditions correspond to the effective aging time, t_e/τ_o, being shortened. This is demonstrated by combining Eq. (9) and (11) to give

$$\ln\tau_o = \frac{-\Delta h^*}{RTg} + \frac{x\Delta h^*}{RT_e} + \frac{(1-x)\Delta h^*}{RT_f'} \qquad (18)$$

where τ_o(Tg) has been put equal to 1 sec and the dependence of τ_o on t_e has been neglected for simplicity. Since $T_f' \approx Tg$,

$$\ln\tau_o \sim \frac{x\Delta h^*}{R}\left(\frac{1}{T_e} - \frac{1}{Tg}\right) \qquad (19)$$

from which it is clear that increasing x and Δh^* and decreasing T_e all lengthen τ_o and thus shorten the effective aging time t_e/τ_o.

We conclude this section with a curious result associated with the effects of Δh^*. For linear relaxations in which the relaxation time is an Arrhenius function of temperature, and the functional form of the decay function is independent of temperature, the variable ln τ_o (ln ω in the frequency domain) is equivalent to $\Delta h^*/RT$. The temperature range of a

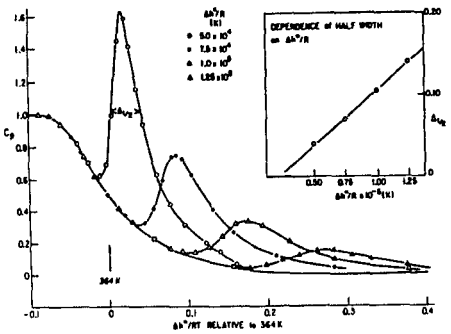

Figure Six Effect of Δh^* on aging peaks. $QC = 10^3$, $QH = 20$, $t_e = 1$ week, $T_e = 313K$, $\beta = 0.25$, $x = 0.35$.

relaxation is therefore a function of Δh^* and it is of interest to see if such scaling occurs for nonlinear relaxations. Calculated C_p^N curves for different values of Δh^* (from ref. 25) are plotted as a function of $\Delta h^*/RT$ in Fig. 6. The glass transition "background" is independent of Δh^* when plotted in this way but the aging peaks are not: their width at half height is a linear function of Δh^* (Fig. 6 inset). The linear relation is not understood, but the general phenomenon appears to be analogous to the superposition of volume maxima on a smoothly decaying background for different aging treatments [Kovacs (51)].

4. Parameter Optimization and Fitting Experimental Data

Before comparing calculated and experimental results it is necessary to normalize the experimental data. The normalized heat capacity $C_p^N(T)$ is given by

$$C_p^N(T) = \frac{Cp(T) - Cpg(T)}{Cp_l(T) - Cpg(T)} \qquad (20)$$

where Cp, Cp_l, and Cpg are the measured liquid and glassy heat capacities respectively. Linear extrapolations of Cpg and Cp_l are made into the transition range, and it is important that the heat capacity be measured far outside the transition region to accurately assess the temperature dependences of Cpg and Cp_l.

The fictive temperature immediately before heating, T_f', is obtained by integrating $C_p^N(T)$, measured during heating, from well below to far above the transition range. The fictive temperature of the glass is obtained from the temperature axis intersection of the extrapolated high temperature integral (a straight line with unity slope). For this analysis it is desirable to keep the heating rate constant so that calibration of the DSC instrument is needed for only one heating rate. The experimental $C_p^N(T)$ data are evaluated every 1K and a computer file containing C_p^N over a 100K temperature range is created. For calculations using dynamically varying temperature steps (Eq. 17), which produce data at non-integer temperatures, values of C_p^N at integral temperatures are obtained by linear interpolation.

The Marquardt optimization procedure (45) was used by Hodge (22) and Hodge and Huvard (21) to obtain the best fit model parameters (A, Δh^*, x, β) from experimental data. The FORTRAN program for the Marquardt procedure was a modified version of that given by Kuester and Mize (46) and worked well in this application. The objective function ψ was

$$\psi = \sum_T [C_p^N(T) - \hat{C}_p^N(T)]^2$$

where C_p^N and $\hat{C}_p^N$ are the experimental and calculated values of $C_p^N(T)$. This objective function has the advantage of placing the least weight on the smallest values of C_p^N, which have the greatest uncertainties because of uncertainties in Cpg. The initial trial values of x and β were 0.5 and the initial value of A was calculated from Eq. 11 with $\ln \tau_o = 1.0$ at Tg. The best fit values of x and β were constrained to lie between 0.001 and 1.0 and lnA was restricted to ±15 of the initial estimate. The values of QC, T_e, t_e, QH, Tg (defined for convenience as the temperature at which C_p^N=0.5), and Δh^* were input. The output consisted of best fit values for x, β, A, and ψ. The value of Δh^* was obtained either from the cooling rate dependence of T_f' (Eq. 10), or from the minimum in ψ as a function of input Δh^*. In all cases for which comparisons could be made, the two evaluations of Δh^* were in reasonable agreement (±20%). In one case, discussed below, agreement was within 5%.

For PVC ψ is determined more by the glass transition data than the sub-Tg peaks, and the optimization failed because the glass transition for PVC is broad and not easily reproduced. In this case, x and β were obtained by matching $C_{p\,max}^N$ and T_{max} of the sub-Tg peaks for several aging times at a single aging temperature (see 5.1.1 for details).

5. Comparison of Calculated and Experimental Results

5.1 Thermal Histories

5.1.1 Poly(vinyl chloride) PVC. The value of Δh^* for PVC obtained from the cooling rate dependence of T_f' (Eq. 10) is 450 kcal $mole^{-1}$ (25). The Tg of ca 363K (C_p^N=0.5, QC=40, QH=10) gives lnA(sec) = -619.0. For the aging studies, very rapid quenching was needed to accelerate the development of sub-Tg

TABLE I

Fit to Aging Data for PVC

($\Delta h^* = 450$ kcal mole^{-1}, ln(A,sec) = -619.0, x = 0.11, $\beta = 0.25$, QC = 2×10^4K min^{-1}, QH = 20K min^{-1})

T_e, °C	t_e, hr	Cp^N_{max}		T_{max}	
		obsd	calcd	obsd	cald
20	7	0.13	0.08	324	323
	27	0.14	0.12	328	327
	150	0.21	0.21	332	333
40	6	0.16	0.19	336	337
	24	0.33	0.31	341	341
	50	0.40	0.40	343	343
60	1	0.21	0.37	351	350
	7	0.66	0.76	357	355
	24	1.10	1.20	359	357
	50	1.60	1.60	360	359

peaks. This was achieved by pouring PVC powder (containing agglomerates of ca 1 μm diameter particles) at ca 120°C into liquid nitrogen. Boiling of the nitrogen stopped after about 2 sec. Assuming Newtonian cooling (exponential decrease in temperature from ca 400K to 77K in 2 sec), a cooling rate through Tg of 2×10^4K min^{-1} was estimated. Aging at 40°C was analyzed to obtain values of x and β which gave the best overall fit to Cp^N_{max} and T_{max} for aging times of 6, 24, and 50 hours. The best fits were obtained with x=0.11, β=0.25. Interestingly, the value of β is the same as that obtained from dielectric data (47). Although it is not expected that dielectric and enthalpy relaxation parameters would be exactly the same, the unusually small values of β for both properties lends credence to the enthalpy relaxation analysis. The best fit parameters and a comparison of experimental and calculated values of Cp^N_{max} and T_{max} for several aging times at three aging temperatures are summarized in Table I. The agreement is within experimental uncertainty, and it is shown below that the parameters in Table I also give a good account of the effects of non-thermal histories on aging at room temperature.

The value of Δh^* for PVC is very high, about four times larger than typical carbon-carbon bond energies. This suggests that at least five chain segments are involved in a relaxation event. The high value of Δh^* and small value of β contribute to the low T_{max} and well developed sub-Tg peaks (Fig. 4). The small value of x would increase T_{max} but this is evidently outweighed by the opposite effects of β and Δh^*.

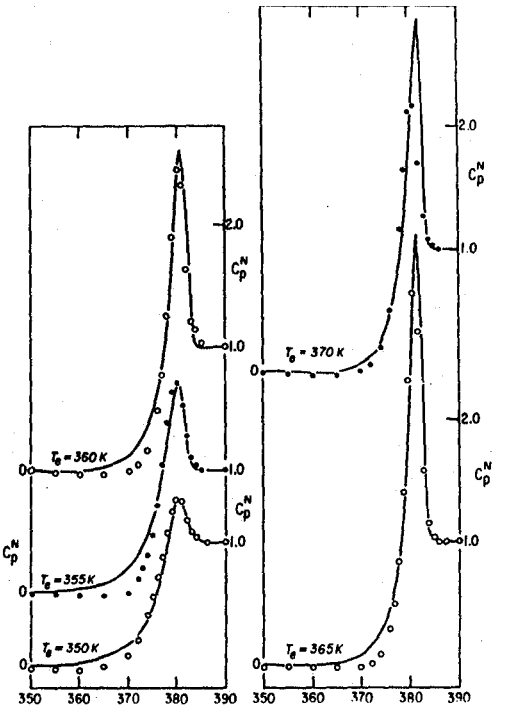

Figure Seven Comparison of experimental (points) and calculated (lines) data for a polydisperse polystyrene (ref 21), after aging for one hour at the indicated temperatures.

5.1.2 Polystyrene (PS). The value of Δh^* for a polydisperse polystyrene (Mw/Mn = 3.8) obtained from the cooling rate dependence of T_f' is 157 kcal mole^{-1} (21). Analysis of a single thermal history with no aging gave a best fit value of 165 kcal mole^{-1} (21), in excellent agreement with the experimental value. Other parameters obtained from analysis of the same thermal history were lnA(sec) = -216.6, x=0.63, β=0.68. These parameters accurately predict the response of Cp^N to other thermal histories, including those with aging, indicating that the glass transition kinetics determine the kinetics of physical aging down to about 30K below Tg (the lowest aging temperature studied). A comparison of experimental and calculated Cp^N is given in Fig. 7. One hour anneals at temperatures down to ca 30K below Tg did not produce sub-Tg heat capacity maxima, in contrast to PVC which exhibited a well developed sub-Tg peak when aged 1 hour about 30K below Tg (see Table I).

Analysis of data obtained by Prest (48) for a monodisperse polystyrene, also for aging temperatures down to ca 30K below Tg, produced a set of parameters similar to that obtained for the polydisperse material (50). However, analysis of data published by Chen and Wang (17) for another monodisperse polystyrene produced parameters which are more like those

TABLE II

Enthalpy Relaxation Parameters

Material	lnA(sec) ±1	Δh* (kcal mole^{-1}) ±10%	x ±0.05	β ±0.05	Reference
PVAc	-275.4	175	0.28	0.53	22
PVAc	-223.6	142.6	0.41	0.51	49
PVC	-619.0	450	0.11	0.25	25
PS	-216.4	165	0.43	0.68	21
PS	-457.0	350	0.12	0.39	21
PMMA	-355.7	275 (±20%)	0.22 (±0.1)	0.37 (±0.1)	22
PCarb	-353.6	300	0.22	0.54	22
As_2Se_3	-85.5	81.8	0.49	0.67	36
B_2O_3	-75.6	90	0.40	0.65	35
5P4E	-153.1	77	0.40	0.70	36

for PVC than for the two PS materials just discussed (Δh^*=350 kcal mole^{-1}, lnA(sec) = -457.1, x=0.12, β=0.39). Although this set of parameters is less reliable because data for only two thermal histories could be analyzed, no single set of parameters could be found which reproduced data for all materials. The parameters for the polydisperse material did not produce the sub-Tg shoulder reported by Chen and Wang under any of several aging conditions which equaled or approximated the experimental conditions. Similarly, the parameters for the monodisperse material did not reproduce the annealing data for the polydisperse material.

The large difference in parameter values for the different polystyrenes is not well understood. However, the low aging temperature for the Chen and Wang experiments (about 60K below Tg) compared with the other experiments (less than 30K below Tg) suggests that the glass transition kinetics give a poor description of aging far below Tg. This is confirmed by analysis of non-thermal histories for PS which involve perturbations at or near room temperature (see §5.2.2 below), which indicate that the Chen and Wang parameters are needed to give a satisfactory account of the data. This contrasts with PVC, for which a single set of parameters gives a good description of aging from Tg down to room temperature. If this difference between PS and PVC with regard to their low temperature aging behavior is real, it is speculated that it reflects the difference in secondary relaxation temperatures (high for PS, low for PVC).

5.1.3 Poly(vinyl acetate) PVAc, Poly(methylmethacrylate) PMMA, Bisphenol A polycarbonate PCarb. Poly(vinyl acetate) has been studied by Sasabe and Moynihan (49) for thermal histories with no aging, and by Hodge (22) for histories with and without aging. There is good agreement between the two sets of parameters (see Table II), and in both cases agreement between experimental and calculated results is comparable with that found for polystyrene (Fig. 7). Polycarbonate was studied by Hodge (22) who again obtained agreement between calculated and experimental data comparable with that found for PS. For PMMA Hodge (22) obtained significantly poorer agreement between observed and calculated data. The parameters for PCarb and PMMA are included in Table II. For all three materials aging temperatures lay between Tg and ca Tg-30K. Thus the possibility exists that, as for PS, different parameters would be obtained from analysis of low temperature aging data.

5.1.4 Correlation of Parameters. A summary of the best fit parameters for materials to which the Moynihan formalism has been applied is given in Table II. An inspection of this table reveals strong correlations between all four parameters, which are displayed in Fig. 8. These correlations are robust with respect to uncertainties in the parameters, as illustrated by the "best fit" parameters for PVAc obtained for values of Δh^* differing by ±15% from the experimental value (Fig. 8). These parameter values move along the correlation lines, so closely in fact that it raises the possibility that the correlations may be generated by the parameter uncertainties. However, the full range of parameters is far greater than the uncertainties and the correlations cannot be eliminated by forcing the parameters to their extreme values. Accordingly the correlations will be accepted as fact for the purpose of discussion.

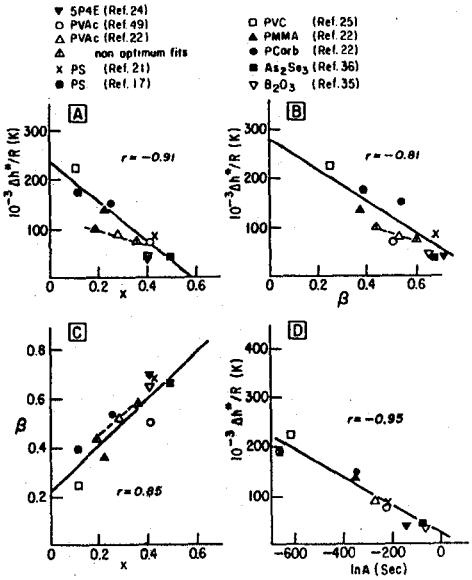

Figure Eight Correlations between best fit parameters for the indicated polymers and inorganic glasses. Nonoptimum parameters for PVAc indicate correlations between parameter uncertainties.

The correlation between A and Δh^* reflects the small range in Tg of the materials listed in Table II. We offer no molecular interpretation of this correlation since it is difficult to attach physical significance to values of A which can be as small as 10^{-270} sec (!!!). The other correlations are consistent with commonly held views on the cooperative nature of the glass transition. To make the discussion concrete, we interpret β as a measure of the number of segments which can move statistically independent of adjacent segments (smaller values of β correspond to a larger number of segments). It is speculated that this number corresponds to a correlation length for some form of fluctuation. The involvement of many chain segments is expected to give a large activation energy, thus accounting for the inverse correlation between β and Δh^*. As noted above for PVC, the large activation energies for most polymers exceed C-C bond energies and therefore also demand the involvement of several chain segments. Relaxation events in which a larger number of chain segments participate might also be expected to be more affected by the molecular environment (i.e. "structure"). To the extent that the parameter x reflects the importance of molecular structure, relative to temperature, in determining the average relaxation time an inverse correlation between x and the number of chain segments per relaxation event might also be expected. This could account for the correlations between x, β and Δh^*. These speculated relations between the number

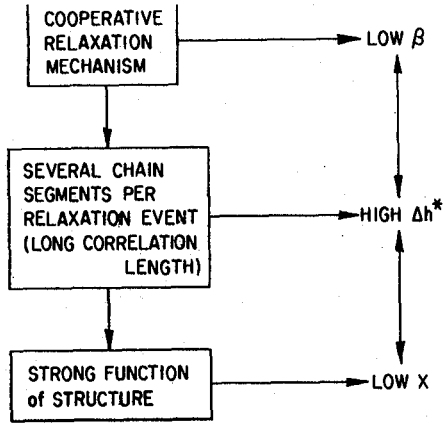

Figure Nine Schematic of speculated relations between model parameters and number of chain segments per relaxation event.

of chain segments per relaxation event and the parameters β, Δh^*, and x are summarized in Fig. 9. Many more data on many more materials are needed to establish the generality of these correlations.

5.2 Preaging Non-Thermal Histories

Several studies of the effects of non-thermal perturbations on physical aging have been reported. We restrict ourselves here to the effects of hydrostatic pressure, mechanical stress, and vapor absorption. In this section we discuss the effects of perturbations which are removed before aging; studies in which the perturbations are maintained during aging are considered in section 5.3.

5.2.1 Hydrostatic Pressure. We discuss two experimental investigations, of PVC (16,39) and PS (4). In both studies pressure was applied above Tg, maintained during cooling to the glassy state, and released before aging and reheating. The experimental heat capacity data of Prest and coworkers (16) for PVC, obtained after aging for 110 days at room temperature and atmospheric pressure, are shown in normalized form in Fig. 10a. The glass transition moves to slightly higher temperatures with pressure and the sub-Tg peak becomes sharper and more assymetric and moves to somewhat lower temperatures. Weitz and Wunderlich (4) studied the effects of hydrostatic pressure applied during cooling on enthalpy relaxation in PS, PMMA and the non-polymeric glasses phenolphthalein, sucrose, and $KNO_3/Ca(NO_3)_2$. Their normalized experimental data for PS are shown in Fig. 11a. Each sample was cooled at 0.083K min^{-1} under various pressures, transferred to the DSC instrument, and heated at 5K min^{-1} at atmospheric pressure. In some cases samples were

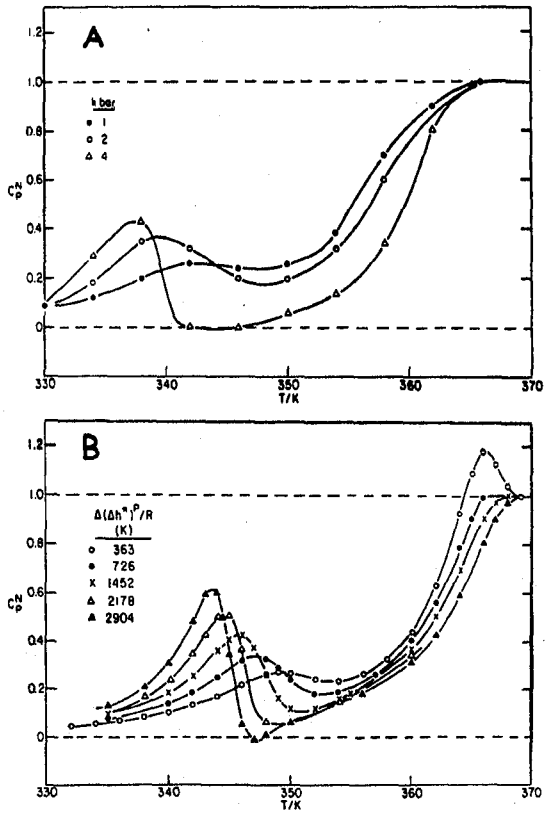

Figure Ten C_p^N data obtained at atmospheric pressure for PVC formed by cooling under the indicated hydrostatic pressures, and aged for 110 days at room temperature. (A) Experimental data after Prest and Roberts (16). (B) Calculated data using the calculation procedure $\Delta P \sim \Delta(\Delta h^*)^P$ (see text).

stored at -10°C for an unspecified time (presumably days or more) before scanning. Physical aging was not deliberately investigated in this study, but probably occurred during transfer of the sample to the DSC instrument and/or during storage at -10°C. For calculation purposes these conditions were assumed to correspond to aging at 300K for 1 second.

Hydrostatic pressure P can be introduced into the calculation procedure in three equivalent ways. All start from the observation that P increases Tg by lengthening the average relaxation time, and all assume the parameters x and β to be independent of pressure. In the first method, the fictive temperature is decreased so that $T_f<T$ at equilibrium when P>0. In the second method the preexponential parameter A is increased with P. Equivalent changes (Δ) in T_f and lnA are related by

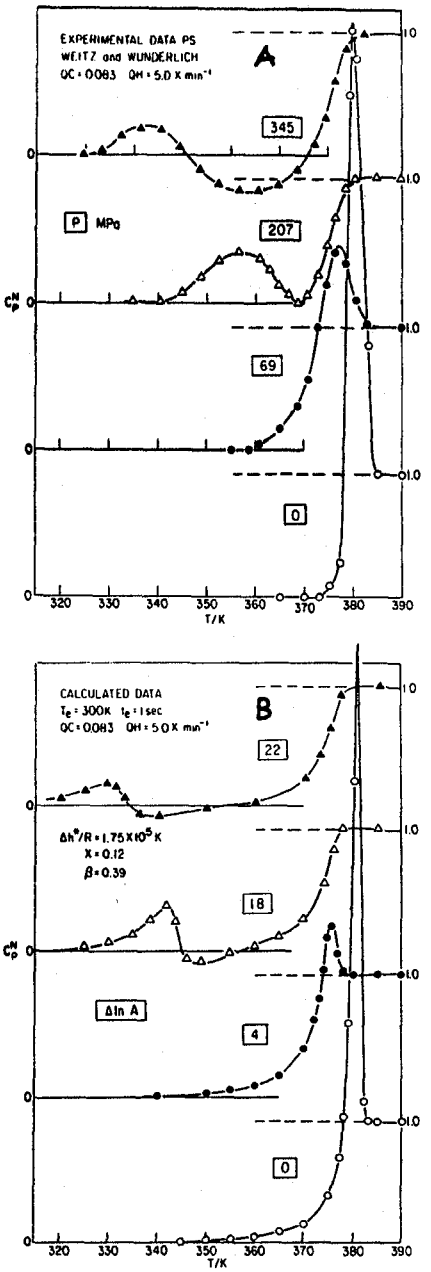

Figure Eleven C_p^N data obtained at atmospheric pressure for PS formed by cooling under hydrostatic pressure. (A) Experimental data after Weitz and Wunderlich (4). (B) Calculated data after aging 1 second at 300K, using calculation procedure $\Delta P \sim \Delta \ln A^P$ (see text).

$$\Delta \ln A^P \sim \frac{(1-x)\Delta h^*}{RTg^2} \Delta T_f^P \qquad (21)$$

where the superscript P indicates changes due to pressure. Third, the activation energy is increased with pressure. Equivalent changes in $\Delta \ln A^P$ and $\Delta(\Delta h^*)^P$ are given by

$$\Delta \ln A^P \sim \frac{\Delta(\Delta h^*)^P}{RTg} \qquad (22)$$

An approximate relation between ΔT_f^P and ΔP is readily derived. First,

$$\Delta \left(\frac{\partial H}{\partial P}\right)_T \sim -TV\Delta\alpha \qquad (23)$$

where α is the thermal expansion coefficient and Δ now refers to changes at the glass transition. Inserting the relation $\Delta(dH) = \Delta CpdT$ into (22), and noting that

$$dT_f \sim \left(\frac{x}{1-x}\right) dT \qquad (24)$$

gives

$$\frac{dT_f}{dP} \sim \frac{\Delta T_f^P}{\Delta P} \sim -\left(\frac{x}{1-x}\right) \frac{TV\Delta\alpha}{\Delta Cp} \qquad (25)$$

In order to provide a reasonable test of the calculation procedure it is necessary to evaluate $\Delta T_f^P/\Delta P$. For PVC $\Delta Cp \sim 0.07$ cal $gm^{-1}K^{-1}$, $\Delta\alpha \sim 2x10^{-4}$ K^{-1}, V=0.7 gm cm^{-3}, Tg=363K, x=0.11. Inserting these values into Eq. (25) gives

$$\Delta T_f^P/\Delta P \sim 2K \text{ kbar}^{-1} \qquad (26)$$

The experimental pressure range (0-6 kbar) thus corresponds to $\Delta T_f^P \sim 0$-12K. Eq. (21) gives $\Delta \ln A^P \sim 0$-12 for the same range, and $\Delta(\Delta h^*) \sim 0$-8.7 kcal $mole^{-1}$. Calculated normalized heat capacities are shown in Fig. 10b for $\Delta(\Delta h^*)^P$; the parameters are those obtained from analysis of purely thermal histories for another PVC (Table II). The calculated curves using ΔT_f^P and $\Delta \ln A^P$ are very similar to those shown in Fig. 10b. Although only qualitative reproduction of experimental trends was aimed for in these calculations, the agreement is quantitatively very good.

To reproduce the PS data it was necessary to use the parameters obtained from the 320K annealing data of Chen and Wang (17) (see Table II). Insertion of the appropriate quantities onto Eq. (25) gave $\Delta T_f^P/\Delta P \sim 2K$ $kbar^{-1}$ $\sim 2x10^{-2}K$ MPa^{-1}. Eqs. (21)$_P$ and (22) give values of 1.1 $kbar^{-1}$ for $\Delta \ln A^P$ and 0.82 kcal $mole^{-1}$ $kbar^{-1}$ for $\Delta(\Delta h^*)_P$. As for PVC, calculations using ΔT_f^P, $\Delta \ln A^P$, and $\Delta(\Delta h^*)$ gave comparable results. Calculated results using $\Delta \ln A^P$ are shown in Fig. 11b. The experimental trends are qualitatively reproduced, namely a decrease in overshoot at low pressures, the development of a sub-Tg peak at intermediate pressures, and the development of an exothermic minimum between T_{max} and Tg at the highest pressures. Similar trends were observed experimentally by Yourtee and Cooper (40) and by Dale and Rogers (43). In view of uncertainties in the experimental aging history and in the parameters for PS, the overall good agreement between calculated and experimental curves is regarded as indicating the essential correctness of the calculation procedure. The calculations indicate that significant room temperature/atmospheric pressure aging occurs in seconds for glasses prepared under high hydrostatic pressure, because of the small values of τ_ρ following pressure release. The sub-Tg peaks observed experimentally for PS are evidently physical aging peaks with the aging occuring during sample transfer from the pressure cell to the DSC instrument.

Data for nonpolymeric glasses exhibit a simple reduction in overshoot with pressure with no sub-Tg peaks occuring, according to Weitz and Wunderlich (4). Insertion of parameters typical of nonpolymeric glasses (e.g. those for 5P4E listed in Table II) produced similar results - no sub-Tg peaks were calculated to occur.

An interesting feature of the calculations for both PVC and PS is that shortened relaxation times in the glassy state are produced only after pressure release; the relaxation time before pressure release is longer than that for the atmospheric pressure vitrified glass. This implies that aging under pressure would be slow, which is observed experimentally (see 5.3).

5.2.2 Mechanical Stress and Vapor Induced Dilation. The effects of mechanical stress of various kinds (cold drawing, powder compaction) on physical aging and enthalpy relaxation in polymers have been observed by several investigators. The general effect is to accelerate aging. Several types of vapor and liquid adsorption and desorption treatments also hasten physical aging (14,20). The discussion here is restricted to data obtained by Berens and Hodge (20) for PVC, which are representative.

The influence of mechanical stress on aging is typified by data for PVC film which was slowly cooled (about 40K min^{-1}) and then cold drawn beyond the yield point (to about 100% elongation). Samples were aged at 40°C for up to 140 hours. Sub-Tg heat capacity peaks developed faster than in liquid nitrogen quenched PVC powder (estimated cooling rate $2x10^4$K min^{-1}, see ref. 20 for details). These data are included in Fig. 12 as plots of Cp_{max} and T_{max} vs log t_e. The effects of swelling by absorbed penetrant are represented by aging data for PVC powder which was cooled at about 40K min^{-1}, swollen by absorption of methyl chloride to a concentration sufficient to depress Tg below room temperature, and vitrified by rapid desorption of the penetrant (in a few seconds, see ref. 20 for details). The rate of sub-Tg peak development in this material, after aging at 40°C, was comparable with that observed for the liquid nitrogen

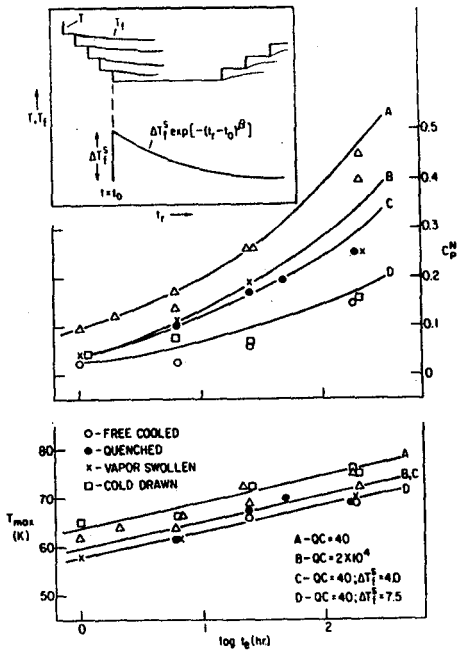

Figure Twelve Experimental (points) and calculated (lines) values of Cp^N_{max} and T_{max} vs log t_e, for PVC with the indicated preaging perturbations. Experimental data after Berens and Hodge (20). Inset: Schematic of calculation procedure.

quenched powder. These data are also displayed in Fig. 12.

Mechanical stress and vapor induced dilation are introduced into the calculation procedure in the same way. An instantaneous increase in T_f', ΔT_f^S, is assumed to occur as a result of the treatment, which decays with aging time and reheating according to

$$\Delta T_f^S(t_r) = \Delta T_f^S \exp[-t_r^{\beta}] \qquad (27)$$

where t_r is the reduced time given by Eq. (12). This is superimposed on the response to the thermal history, Eqs. (14),(15). The two responses are coupled by their common dependence of τ_o on T_f. It is assumed that the model parameters are unaffected by cold drawing or swelling. The calculation procedure is displayed schematically in Fig. 12 inset.

A comparison of calculated and experimental data requires that ΔT_f^S be evaluated. Its value was obtained by matching the calculated and smoothed experimental values of Cp^N_{max} for an aging time of 24 hours at 40°C. The calculations are tested by comparing predictions of Cp^N_{max} for other aging times, and T_{max} for all times, with experiment. The calculated curves are shown as the solid lines in Fig. 12, and are in good overall agreement with experiment. In particular the experimental result that the vapor swollen and liquid nitrogen quenched powders age almost identically is reproduced. This is in apparent disagreement with the memory effects associated with a nonexponential decay function. However, the important concept in the memory effect is the reduced time taken to reach the starting value relative to the reduced evolution time. In both the liquid nitrogen quenched and vapor dilated glasses the elevated enthalpy at the start of aging is reached (from the equilibrium state above Tg) essentially instantaneously compared with the aging time.

TABLE III

Effects of Hydrostatic Pressure Applied During Aging of PVC

Hydrostatic Pressure (MPa)	ΔT_f^P	Cp^N_{max} obsd	Cp^N_{max} calcd	T_{max} obsd	T_{max} calcd
0	0	0.14	0.18	341	345
47	-2	0.07	0.11	333	332
94	-4	0.04	0.04	320	321

The good agreement of calculated and experimental results exhibited in Fig. 12 indicates that the calculation procedure is essentially correct. In particular, the agreement justifies the assumption that the model parameters are not affected by possible structural or conformational changes induced by cold drawing or methyl chloride plasticization.

5.3 Co-Aging Nonthermal Histories

The effects of hydrostatic pressure, tensile stress and vapor adsorption applied during aging, on enthalpy relaxation in PVC, have been investigated by Berens and Hodge (44). In all cases the development of sub-Tg peaks is slowed down, corresponding to a lengthening of the average relation time. The peak temperature, T_{max}, generally decreases although in some cases this is not evident until large perturbations are applied. The discussion here is restricted to the effects of approximately hydrostatic pressure, applied by a plunger to powdered PVC. The powder was cooled at about 40K min^{-1} at atmospheric pressure before aging for 24 hours at 40°C under several pressures. A summary of Cp^N_{max} and T_{max} as a function of applied pressure is given in Table III.

The calculation procedure for coaging perturbations was to decrease T_f by an amount ΔT_f^P during aging, or to increase A or Δh^* by a constant amount during aging. As before, the parameters x and β are assumed to be unaffected by pressure. This procedure guarantees

that ΔH_e will diminish with pressure, so that barring an extreme narrowing of the sub-Tg peak Cp^N_{max} will also decrease. The accuracy of the calculation is assessed from the shift in T_{max}, and an assumed monotonic increase in the magnitude of ΔT_f with pressure. Calculated values of Cp^N_{max} and T_{max} are compared with experimental values in Table III. The agreement in T_{max} is very good and there is an almost linear increase in ΔT_f, $\Delta \ln A$, and $\Delta(\Delta h^*)$ with P. This agreement again indicates that the calculation procedure is essentially correct.

6. Summary and Conclusions

The effects of physical aging on enthalpy relaxation in polymers are generally well described by the phenomenology used to characterize the glass transition kinetics. The development of sub-Tg heat capacity maxima with aging in some materials, most notably PVC, has been shown to reflect the nonexponential decay function for enthalpy relaxation. The effects of nonthermal perturbations such as hydrostatic pressure, mechanical deformation, and vapor induced dilation can be calculated by simple extensions to the standard phenomenology. Perhaps surprising is the apparent invariance of the four parameters (A, Δh^*, x, and β) with respect to temperature, pressure, deformation, and departure from equilibrium. It is known that these invariances are approximate but evidently any variations are incidental to, and not causative of, the enthalpic manifestations of physical aging. The correlations between the four parameters observed for several polymers need to be investigated in more detail. The success of the Marquardt optimization procedure for obtaining enthalpy relaxation parameters from experimental data should allow testing of correlations for a large number of materials, including but not restricted to other polymers. If the correlations successfully withstand further studies, a common physical origin for all the parameters would be indicated. A possible candidate is the number of chain segments per relaxation event, or perhaps a correlation length for fluctuations in conformation or similar measure of molecular structure.

Acknowledgments

It is a pleasure to thank D. Puraty and F. Kunig for their experimental assistance, and G. Huvard for his contribution to the Marquardt optimization studies. I thank A. R. Berens, H. B. Hopfenberg, W. M. Prest, Jr. and J. M. O'Reilly for many helpful comments. Much of the work described here was supported by the National Science Foundation under the Industry-University Cooperative Research Program through Grant No. CPE-7920740. I thank The BFGoodrich Company for permission to publish.

References and Notes

1. K. H. Illers, Makromol. Chem. 127 1 (1969).
2. M. V. Volkenstein and Yu. A. Sharonov, Vysokomol. Soed 3 1739 (1961).
3. C. R. Foltz and P. V. J. McKinney, J. Appl. Sci. 13 2235 (1969).
4. A. Weitz and B. Wunderlich, J. Polym. Sci. Polym. Phys. Ed. 12 2473 (1974).
5. A. Gray and M. Gilbert, Polymer 17 44 (1976).
6. R. Straff and D. Uhlmann, J. Polym. Sci., Polym. Phys. Ed. 14 1087 (1976).
7. T. E. Brady and S. A. Jabarin, Polym. Eng. Sci. 17 686 (1977).
8. G. Ceccorolli, M. Pizzoli, and G. J. Pezzin, Macromol. Sci. Phys. B14 499 (1977).
9. I. G. Brown, R. E. Wetton, M. J. Richardson, and N. G. Savill, Polymer 19 659 (1978).
10. Z. H. Ophir, J. A. Emerson, and G. L. Wilkes, J. Appl. Phys. 69 5032 (1978).
11. M. J. Richardson and N. G. Savill, Br. Polym. J. 11 123 (1979).
12. J. M. O'Reilly, J. Appl. Phys. 50 6083 (1979).
13. M. G. Wysgoski, J. Appl. Polm. Sci. 25 1455 (1980).
14. A. R. Shultz and A. L. Young, Macromolecules 13 633 (1980).
15. W. M. Prest, Jr., J. M. O'Reilly, F. J. Roberts, Jr., and R. A. Mosher, Polym. Eng. Sci. 21 1181 (1981).
16. W. M. Prest, Jr. and F. J. Roberts, Jr., Ann. N.Y. Acad. Sci. 371 67 (1981).
17. H. S. Chen and T. T. Wang, J. Appl. Phys. 52 5898 (1981).
18. J. Menczel and B. Wunderlich, J. Polym. Sci. Polym. Lett. 19 261 (1981).
19. C. Bauwers-Crowet and J.-C. Bauwens, Polymer 23 1599 (1982).
20. A. R. Berens and I. M. Hodge, Macromolecules 15 756 (1982).
21. I. M. Hodge and G. S. Huvard, Macromolecules 16 371 (1983).

22. I. M. Hodge, Macromolecules 16 898 (1983).

23. U. Yilmazer and R. J. Farris, J. Appl. Polym. Sci. 28 3269 (1983).

24. A. J. Kovacs, J. J. Aklonis, J. M. Hutchinson, and A. R. Ramos, J. Polym. Sci., Polym. Phys. Ed. 17 1097 (1979).

25. I. M. Hodge and A. R. Berens, Macromolecules 15 762 (1982).

26. A. J. Kovacs, Fortschr. Hochpolym. Forsch 3 394 (1963).

27. This function can be traced back to Kohlrausch, but is often referred to as the Williams-Watts function following its application to dielectric relaxation by Williams and Watts [Trans. Faraday Soc. 66 80 (1970)]. It figures prominently in the mathematical modeling of physical aging described in section 3.

28. A. Q. Tool, J. Am. Ceram. Soc. 29 240 (1946).

29. R. Gardon and O. S. Narayanaswamy, J. Am. Ceram. Soc. 53 148 (1970).

30. O. S. Narayanaswamy, J. Am. Ceram. Soc. 51 691 (1971).

31. H. N. Ritland, J. Amer. Ceram. Soc. 37 370 (1954).

32. C. T. Moynihan, A. J. Easteal, and M. A. DeBolt, J. Amer. Ceram. Soc. 59 12 (1976).

33. C. T. Moynihan, A. J. Easteal, J. Wilder, and J. Tucker, J. Phys. Chem. 78 2673 (1974).

34. L. C. E. Struik, "Physical Aging in Amorphous Polymers and Other Materials", Elsevier, New York (1978).

35. M. A. DeBolt, A. J. Easteal, P. B. Macedo, and C. T. Moynihan, J. Amer. Ceram. Soc. 59 16 (1976).

36. C. T. Moynihan et al., Ann. N.Y. Acad. Sci. 279 15 (1976).

37. H. P. Brown, G. M. Musindi, and Z. H. Stachurski, Polymer 23 1508 (1982).

38. R.-J. Roe and G. M. Millman, Polym. Eng. Soc. 23 318 (1983).

39. J. M. O'Reilly and R. A. Mosher, J. Appl. Phys. 51 5137 (1980).

40. J. B. Yourtee and S. L. Cooper, J. Appl. Polym. Sci. 18 897 (1974).

41. R. E. Wetton and H. G. Moneypenny, Br. Polym. J. 7 51 (1975).

42. R. M. Kimmel and D. R. Uhlmann, J. Appl. Phys. 42 4917 (1971).

43. W. C. Dale and C. E. Rogers, J. Appl. Polym. Sci. 16 21 (1972).

44. A. R. Berens and I. M. Hodge, to be published.

45. D. M. Marquardt, J. Soc. Indust. Appl. Math 11 431 (1963).

46. J. L. Kuester and J. H. Mize, "Optimization Techniques with FORTRAN", McGraw-Hill: New York, 1973.

47. I. M. Hodge, unpublished analysis of literature data [Ishida, Y. Kolloid Z. 168 29 (1960)].

48. W. M. Prest, Jr., private communication.

49. H. Sasabe and C. T. Moynihan, J. Polym. Sci. 16 1447 (1978).

50. I. M. Hodge, unpublished results.

51. A. J. Kovacs, J. Polym. Sci. 30 131 (1958).